Journal of Bioenergetics and Biomembranes, Vol. 32, No. 5, 2000

The Catalytic Transition State in ATP Synthase[1]

Alan E. Senior,[2,3] Joachim Weber,[2] and Sashi Nadanaciva[2]

The catalytic transition state of ATP synthase has been characterized and modeled by combined use of (1) Mg-ADP–fluoroaluminate, Mg-ADP–fluoroscandium, and corresponding Mg-IDP–fluorometals as transition-state analogs; (2) fluorescence signals of β-Trp331 and β-Trp148 as optical probes to assess formation of the transition state; (3) mutations of critical catalytic residues to determine side-chain ligands required to stabilize the transition state. Rate acceleration by positive catalytic site cooperativity is explained as due to mobility of α-Arg376, acting as an "arginine finger" residue, which interacts with nucleotide specifically at the transition state step of catalysis, not with Mg-ATP- or Mg-ADP-bound ground states. We speculate that formation and collapse of the transition state may engender catalytic site α/β subunit-interface conformational movement, which is linked to γ-subunit rotation.

KEY WORDS: Oxidative phosphorylation; ATP synthase; F_1-ATPase; catalytic transition state.

INTRODUCTION

In mitochondria, chloroplasts, and bacteria, ATP synthase uses transmembrane proton gradient energy to drive ATP synthesis. In bacteria it can also use ATP hydrolysis energy to generate a transmembrane proton gradient. Energy coupling between catalytic sites located in the F_1 sector and the proton pump machinery in the membrane bilayer is achieved at a distance of around 100 Å by subunit rotation. Direct, visually striking experiments showed physical rotation of subunits γ (Noji *et al.*, 1997), ε (Kato-Yamada *et al.*, 1998), and *c* (Sambongi *et al.*, 1999; Panke *et al.*, 2000; but see also Tsunoda *et al.*, 2000), at the same speed, in response to ATP hydrolysis, indicating that these three subunits together form a rotary transmission device. Proton transport-linked subunit rotation has not yet been experimentally proved, but is generally assumed to occur. How rotation and proton transport are interconverted and how enzymic events in catalytic sites and rotation are integrated, are two major questions.

In order to understand how catalysis in the three catalytic nucleotide-binding sites is integrated with subunit rotation, well-defined and detailed descriptions of the catalytic pathways of ATP synthesis and ATP hydrolysis will be required. This has not yet been achieved and, indeed, remains controversial. The reader is referred to a recent review (Weber and Senior, 2000) for analysis and diagrams of currently proposed mechanisms. In actuality none of the currently available models, or a composite thereof, is of sufficient detail or sophistication to allow an understanding of how ATP synthesis is driven by rotation or how ATP hydrolysis drives rotation. For this, expanded mechanistic models must be developed, that, starting at one point in the catalytic cycle and returning to the same point, include as many defined enzyme intermediate states as possible. New techniques are needed to define and isolate enzyme intermediates, to characterize each intermediate in terms of enzyme structure (*e.g.*, spatial relationship of γ/ε subunits vis-a-vis α/β subunits), and to determine energetic and chemical status along the reaction pathway. Determination of the reaction status of each catalytic site in temporal comparison to the other two sites will also be an important task.

[1] Key to abbreviations: BeFx, beryllium fluoride (fluoroberyllate) (the exact composition of this complex in F_1-ATPase is not yet known, see Henry *et al.*, 1993; Maruta *et al.*, 1993); AlFx, aluminum fluoride (fluoroaluminate) (in different enzymes this has been seen by X-ray crystallography to involve either AlF_3 or AlF_4^- (Schlichting and Reinstein, 1999); Vi, orthovanadate; ScFx, scandium fluoride (fluoroscandium).

[2] Department of Biochemistry and Biophysics, Box 712, University of Rochester Medical Center, Rochester, New York 14642.

[3] To whom all correspondence should be addressed: e-mail: alan_senior @urmc.rochester.edu

0145-479X/00/1000-0523$18.00/0 © 2000 Plenum Publishing Corporation

The catalytic transition state is an important intermediate of any enzyme reaction and is of particular interest in an enzyme engaged in energy coupling. In this paper, we describe work on the transition state of ATP synthase and present proposals as to how it might relate to subunit rotation.

STUDIES OF THE CATALYTIC TRANSITION STATE IN ATP SYNTHASE

Tight Binding Inhibitors Which Mimic and Trap Intermediates of ATPase and GTPase Enzymes

Work on myosin and G-proteins, two of the best-understood NTPase enzymes, has exemplified the major utility of tight-binding inhibitors in establishing the mechanism of catalysis and energy coupling. These inhibitors work by tenaciously trapping the hydrolysis product, NDP, in the catalytic site. For each of these enzymes, much biochemical evidence and several different X-ray structures have been obtained by trapping the enzyme at different stages of the catalytic pathway. Examples of the inhibitors used are fluoroberyllate (BeFx), which mimics the ground-state bound Mg-NTP complex, and fluoroaluminate (AlFx), fluoroscandium (ScFx), and orthovanadate (Vi), all three of which mimic the catalytic transition state (Coleman *et al.*, 1994; Sondek *et al.*, 1994; Fisher *et al.*, 1995; Gopal and Burke, 1995; Smith and Rayment, 1996; Rittinger *et al.*, 1997; Scheffzek *et al.*, 1997; Schindelin *et al.*, 1997; Schlichting and Reinstein, 1997; Tesmer *et al.*, 1997; Xu *et al.*, 1997; Maruta *et al.*, 1998). It has emerged that the catalytic transition state is critically involved at the stage of energy transduction, generating major domain movement in myosin and signaling in G-proteins (Rayment, 1996; Rees and Howard, 1999). Interestingly, the degree of domain movement in myosin was seen to be correlated with the ADP–O to metal bond distance (Park *et al.*, 1997). This distance is 1.57 Å in the ADP–BeFx complex (similar to the ADP–O to γ-phosphorus bond distance in ATP itself), increasing to 2.0–2.2 Å in the transition state with bound ADP–AIFx, ADP–ScFx, or ADP–Vi, exemplifying how subtle changes in spatial separation of the β and γ phosphates of ATP during the chemical reaction may be amplified into larger, distant, conformation changes. The conclusion that energy coupling occurs at the stage of attainment of the catalytic transition state is also supported well in the case of nitrogenase (Rees and Howard, 1999) and P-glycoprotein (Senior *et al.*, 1995, Dey *et al.*, 1997; Ramachandra *et al.*, 1998). Thus, in ATP synthase, it is pertinent to consider how small spatial changes in the catalytic sites, involving ligands that stabilize the transition state, might be amplified into larger conformational movements, including subunit rotation.

Trapping the Catalytic Transition State of ATP Synthase

AlFx was shown to inhibit ATP hydrolysis in the F_1 sector of bovine mitochondrial and *E. coli* ATP synthase by trapping ADP in catalytic sites (Lunardi *et al.*, 1988; Issartel *et al.*, 1991). The inhibition was quasi-irreversible, with a half-time for reactivation of 38 days at 4°C. Two moles of ADP–AlFx were bound per mole F_1. Later work confirmed that ADP–AlFx became bound at two sites cooperatively, although binding at only one site was found sufficient for full inhibition (Dou *et al.*, 1997). A recent F_1X-ray structure shows ADP–AlF_3 bound in just one catalytic site (the βDP site), but the stoichiometry of one mole/mole was thought to be due to loss of ADP–AlFx during crystallization (Braig *et al.*, 2000). A second X-ray structure with ADP-AlFx bound at two catalytic sites and ADP at the third site has also been obtained (A.G.W. Leslie and J.E. Walker, personal communication). In both structures, the ADP–AlFx appears to represent a transition state.

Vi has been shown to inhibit rat mitochondrial F_1-ATPase by trapping ADP. Photochemical activation facilitated by bound Vi cleaved one of the three β subunits, within the Walker A sequence; photoactivation of the myosin–ADP–Vi transition state complex cleaves myosin at the homologous position (Ko *et al.*, 1997). However, we could not detect inhibition of *E. coli* F_1 by Vi (unpublished work). ScFx was shown to inhibit *E. coli* F_1 potently by trapping ADP in catalytic sites, forming an ADP–ScFx complex, which mimics the transition state (Nadanaciva *et al.*, 2000). Reactivation of ATPase activity after ScFx inhibition occurs with a half-time of 12 h at 20°C (with AlFx the $t_{1/2}$ was 100 h). In summary, AlFx, ScFx, and Vi are established as transition-state probes of ATP synthase, with some interspecies variation.

Fluorescence Measurements of Nucleoside Diphosphate Trapped in Catalytic Sites by Fluorometals

β-Trp331 Fluorescence

Use of substituted β-Trp331[4] in the βY331W mutant enzyme (Weber *et al.*, 1993) is an established tool

[4] *E. coli* residue numbers are used.

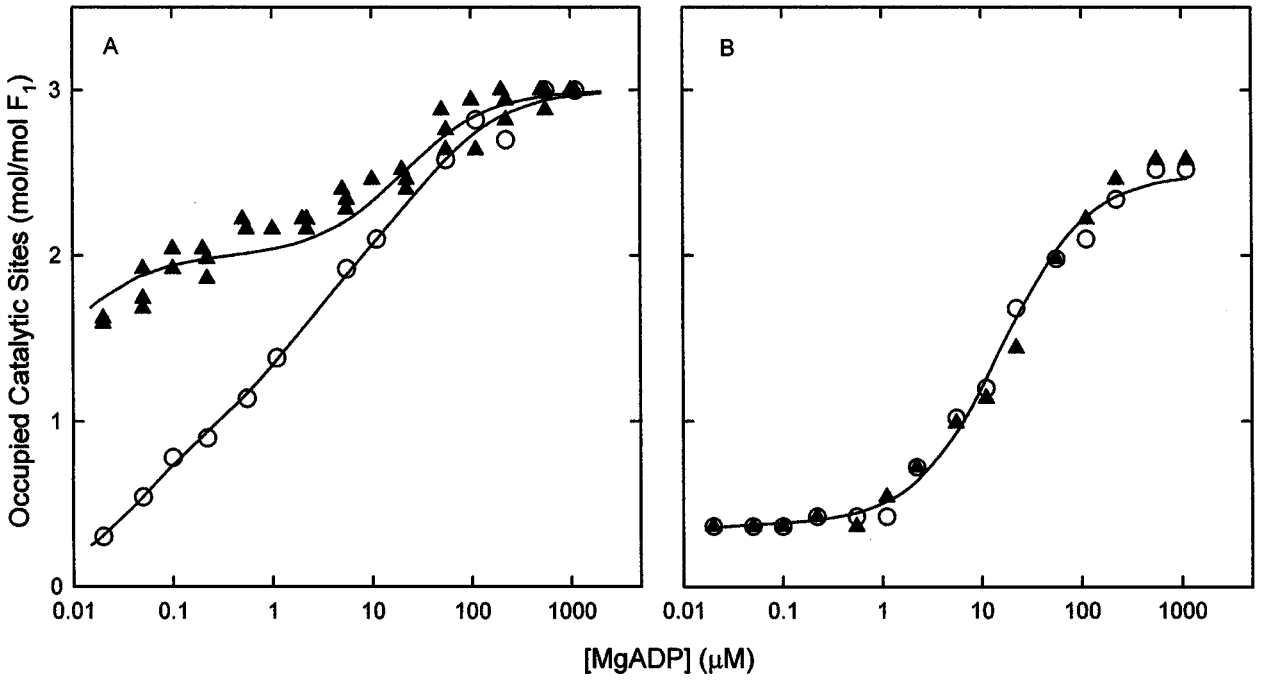

Fig. 1. Combined use of the fluorescence signal of inserted Trp residue β-Trp331, MgADP. ScFx, and mutagenesis of critical catalytic residues, to probe the catalytic transition state. (A) Titration of βY331W mutant *E.coli* F_1 with Mg-ADP in presence (▲) or absence (❍) of fluoroscandium (ScFx). Quench of β-Trp331 fluorescence at 360 nm was measured to monitor nucleotide binding. The lines are fits to a model assuming three binding sites of different affinities. Greatly enhanced affinity for Mg-ADP at catalytic sites one and two is evident in presence of ScFx. (B) Titration of βK155Q/βY331W mutant F_1 with Mg-ADP in presence (▲) or absence (❍) of fluoroscandium (ScFx). Conditions are as in (A). It is evident that removal of the β-Lys155 side chain prevents enhancement of Mg-ADP binding. β-Lys155 is the Walker A Lys, known to be critical for catalysis.

for measurement of nucleotide equilibrium-binding parameters at catalytic sites of F_1. The introduced β-Trp331 has a large fluorescence signal, which is fully quenched upon addition of nucleotide. Titration with Mg-ADP–AlFx demonstrated a very large increase in binding affinity for Mg-ADP at catalytic site 1, with a significant, but less substantial increase at site 2, and no effect at site 3 (Nadanaciva *et al.*, 1999a). Titration with Mg-ADP–ScFx yielded similar data (shown in Fig. 1A) except that in this case the affinity increase was very large at both sites 1 and 2 and, again, site 3 was unaffected (Nadanaciva *et al.*, 2000). Table I shows K_d values obtained. In absence of Mg^{2+}, the fluorometals had no effect on ADP binding. These results were consistent with earlier data showing binding of 2 mol Mg-ADP–AlFx per mole of F_1, They indicate that a transition state certainly forms at the highest affinity site 1 and either a partial or complete transition state can form at site 2, but not at site 3.

Earlier work (Webb *et al.*, 1980; Senter *et al.*, 1983) suggested that the transition state involved a pentacovalent, bipyramidal, phosphorus intermediate; this is buttressed by the fact that Vi, AlFx, and ScFx are potent inhibitors. Such an intermediate requires stabilization by ligands to the equatorial oxygens and an apically bonded water. X-ray structures (Abrahams *et al.*, 1994; Bianchet *et al.*, 1998) had given strong clues where to look for side chains that stabilize the transition state and previous mutagenesis experiments had already revealed critical catalytic residues. A series of appropriate mutations were combined with βY331W and the resultant double-mutant F_1 preparations were examined for Mg-ADP binding in presence of AlFx or ScFx. An example is given in Fig. 1B, where it is seen that the βK155Q mutation totally eliminates the

Table I. Binding of Mg-ADP to Catalytic Sites of *E. coli* F_1 and Its Enhancement by AlFx and ScFx[a]

Ligand	K_{d1} (μM)	K_{d2} (μM)	K_{d3} (μM)
Mg-ADP	0.04	1.8	34.8
Mg-ADP–AlFx	<0.001	0.06	40.0
Mg-ADP–ScFx	<0.001	<0.01	20.5

[a] Binding parameters were calculated from fits to titration curves as shown in Fig. 1A.

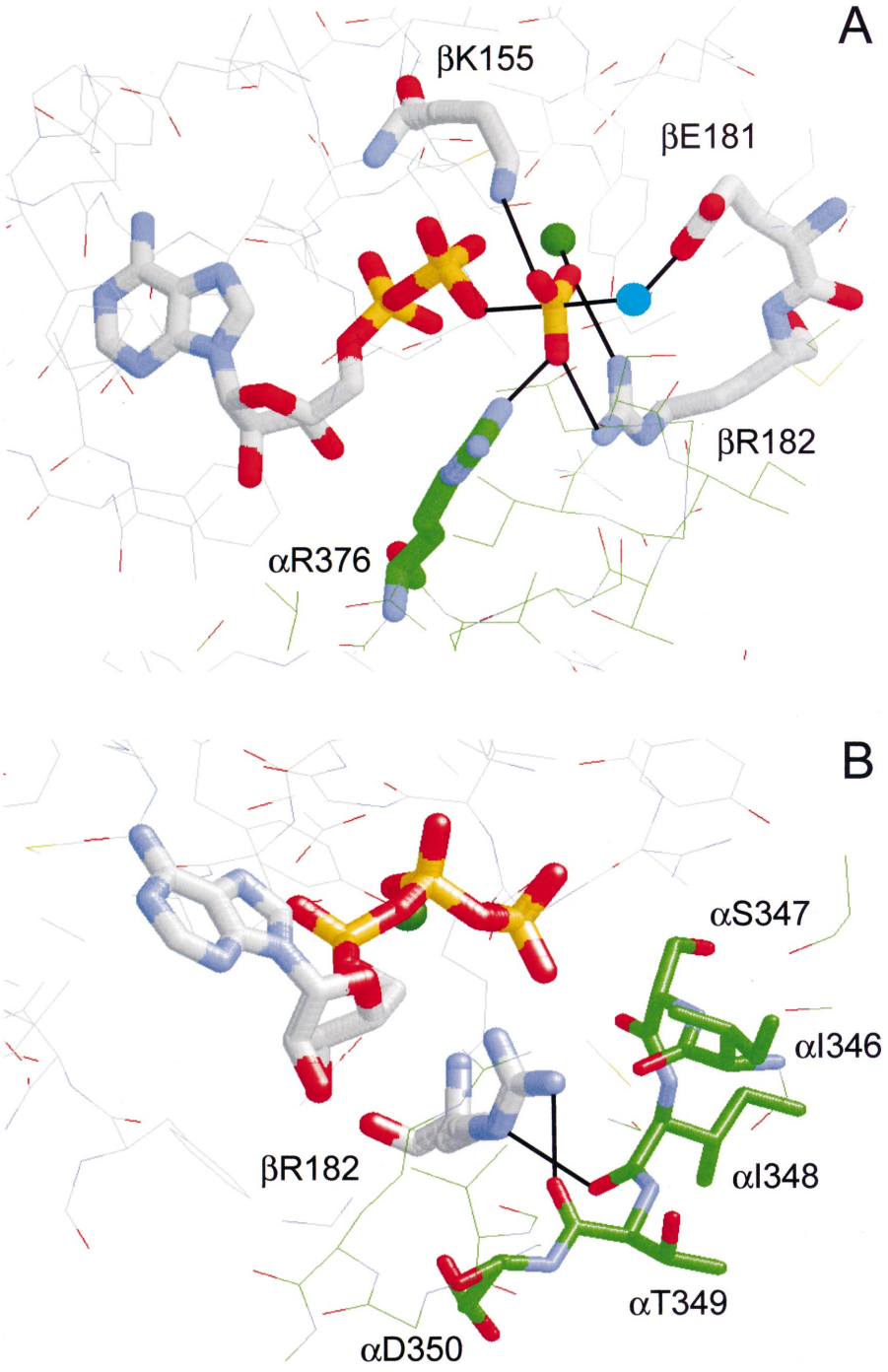

Fig. 2. The catalytic transition state of ATP synthase and the catalytic α/β subunit interface. (A) Model of the catalytic transition state of ATP synthase. α-Subunit residues are shown in green, β subunit residues are shown in grey; Mg^{2+} is the green sphere, the attacking water is cyan. (B) The α/β subunit interface. α-Subunit residues are shown in green and β-subunit residues are shown in grey. Possible H-bonds between β-Arg182 and main chain carbonyl oxygens of α-Ile348 and α-Thr349 are shown in black. We postulate that β-Arg182 may amplify small conformational movements generated at the transition state into larger α/β subunit interface conformational movements. As noted in the text, α-Arg376 may play a similar role.

effect of ScFx to increase Mg-ADP binding affinity at catalytic sites 1 and 2. Using this approach, we identified four residues that are critical for transition-state stabilization and proposed a model for the transition state shown in Fig. 2A. The X-ray structure of the Mg-ADP–AlF_3 transition state (Braig *et al.*, 2000) concurs with the model. It may be remarked that the finding that βE181Q mutation abolishes transition-state formation provides independent evidence for an associative mechanism of hydrolysis. In addition to ligands to the phosphate oxygens and the attacking water, ligands orienting Mg^{2+} are also critical for catalysis and transition-state formation, although not shown in Fig. 2A. These are β-Thr156, β-Glu185, and β-Asp242 (Weber *et al.*, 1998).

β-Trp148 Fluorescence

We found that the fluorescence signal of β-Trp148 in the βF148W mutant was enhanced by +28% upon addition of Mg-ADP–AlFx or Mg-ADP–ScFx (see Fig. 3), providing the first direct optical probe of the transition state. Just as Mg-lDP binds less tightly than Mg-ADP (by a factor of about 100-fold), so the Mg-lDP–fluorometal complexes were found to bind less tightly than the corresponding Mg-ADP–fluorometal complexes, while yielding the same +28% fluorescence enhancement of β-Trp148. This was useful experimentally, because it allowed us to determine whether the whole enhancement was due to binding at just site one, or to binding at sites one and two. Titration with Mg-lDP–AlFx and Mg-lDP–ScFx demonstrated that approximately half of the β-Trp-148 fluorescence enhancement occurred upon filling of site 1, the other half was realized upon filling of site 2, and no further increase occurred on filling of site 3 (Nadanaciva *et al.*, 2000).

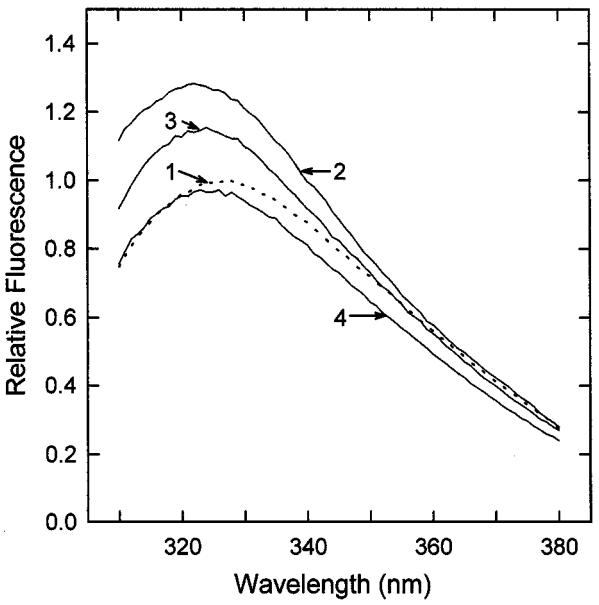

Fig. 3. The fluorescence signal of inserted β-Trp148 provides a direct optical probe of the transition state. Fluorescence spectra of βF148W mutant *E.coli* F_1 are shown. (Curve 1) dotted line: βF148W F_1 alone; (Curve 2) βF148W F_1 with Mg-ADP–ScFx; (Curve 3) βF148W F_1 with Mg-AMP–PNP; (Curve 4) βF148W F_1 with Mg-ADP.

Two Sites Can Assume a Transition State Conformation Simultaneously?

The work described above leads to the conclusion that two catalytic sites can form a transition state conformation simultaneously. This appears to contradict accepted dogma that in the ATP synthase catalytic mechanism, only one site is catalytically active at any one time. All current postulated mechanisms make this assumption (Weber and Senior, 2000). Of course, it need not be that sites 2 and 2 contribute equally to turnover, even if both are active simultaneously—they differ considerably in nucleoside diphosphate–fluorometal binding affinity, for example (Table I). It could also be that AlFx and ScFx are forcing the second site into a conformation that it would not normally assume, at least until it undergoes the "binding change." Nevertheless, this work introduces a new conceptual aspect into study of the ATP synthase mechanism.

Positive Catalytic Cooperativity

F_1 hydrolyzes Mg-ATP in three different modes. The first is by unisite catalysis, when Mg-ATP occupies a single site, and a single turnover event occurs with bond cleavage rate of 0.1 s^{-1}, and net turnover rate of 0.001 s^{-1}, because of slow product release (Al-Shawi and Senior, 1992). The second is by bisite catalysis, where two sites are occupied by Mg-ATP, yielding a net turnover rate of around 1 s^{-1}; the third is the physiological (V_{max}) mode, with all three sites occupied by Mg-ATP, occurring with net turnover rate of around 100 s^{-1} (Weber *et al.*, 1993; Löbau *et al.*, 1998). True rate constants for the bond cleavage step are not known for bi- and trisite catalysis, however, it is obvious that acceleration from unisite mode to V_{max} requires at least 10^3-fold acceleration of the chemical bond-cleavage rate. This strong positive catalytic cooperativity requires that the transition state must change in structure to effectuate rate acceleration from unisite up to V_{max} rate. We found that residue α-Arg376 does not interact directly with nucleotide in either the

Mg-ATP-or Mg-ADP-bound ground states, but is required for Mg-ADP–AlFx and Mg-ADP–ScFx binding, and we proposed (Nadanaciva *et al.*, 1999c) that α-Arg376 inserts into the catalytic site specifically to contribute to stabilization of the transition state, analogous to the "arginine finger" residues of G-proteins and their cognate GAPs. Support for this idea comes from two other sources First, in the F_1 X-ray structure, significant movement of α-Arg376 occurs between βDP and βTP sites, showing that this residue is mobile (Abrahams *et al.*, 1994); second, in recent work it was found that mutations of residue α-Arg376 abolish steady-state catalysis, but have no effect on unisite catalysis (Le *et al.*, 2000). Thus, α-Arg376 is not involved in the unisite transition state, but moves into the catalytic site to form the complete V_{max} transition state. It is, therefore, a major, perhaps sole, determinant of positive catalytic cooperativity.

Role of the Catalytic α/β Interface in Catalysis

Nearly all the direct ligands to bound nucleotide in catalytic sites are derived from β-subunit residues. Nevertheless, X-ray structures show that the catalytic sites occur at α/β subunit interfaces, with bound nucleotide facing the α subunit across a cleft. Conformational movement at the α/β subunit interface has long been known to be essential for positive catalytic cooperativity and steady-state catalysis. The evidence for this was derived from studies of a number of mutants in which small α-subunit residues were changed to bulky residues (αG351D, αS373F, αS375F, and αS373C reacted with NEM). The X-ray structures demonstrate that these residues line the α/β catalytic site interface. Figure 9 of Weber and Senior (1997) shows the α/β catalytic interface and the position of these mutations, and the same reference describes their functional effects in detail. In these mutants, unisite catalysis is unimpaired, but steady-state catalysis is abolished, while catalytic site Mg-ATP and Mg-ADP cooperative binding characteristics remain unchanged. An analysis of potential steric clashes using the tool "Swiss-PdbViewer" (Guex and Peitsch, 1997) reveals that αG351D, αS373F, and αS375F all engender serious clashes with nearby α-subunit residues at the α/β interface of the βDP site. α-Arg376 is contiguous with these mutation sites and a likely scenario is that introduction of additional bulk by mutation impedes movement of α-Arg376 toward the catalytic site-bound nucleotide to form the transition state (Fig. 2A). Thus acceleration of unisite to steady-state catalysis rate cannot occur. α/β interface conformational movement can be seen to be directly linked through α-Arg376 to transition-state formation. Since unisite catalysis does not involve rotation (Garcia and Capaldi, 1998), whereas steady-state catalysis does, α/β conformational movement is also correlated to rotation.

Residue βR182 is also a stabilizing ligand of the transition state (Fig. 2A). Studies of the mutants βR182Q and βR182K revealed that while both inhibited steady-state catalysis stongly, there were differential effects on transition-state stabilization, with the latter mutant appearing to support normal transition state formation as judged by Mg-ADP–AlFx binding (Nadanaciva *et al.*, 1999b). Scrutiny of the X-ray structure showed that the β-Arg182 guanidinium lies close to the α/β interface, within H-bonding distance of αThr349 and α-Ile348 main chain carbonyl oxygens (see Fig. 2B). Thus β-Arg182 may play a dual role, namely transition-state stabilization and interaction with the α subunit to generate α/β interfacial conformational movement. We speculate that the βR182K mutant supports the former, but not the latter function. Proximity of the α-Arg376 guanidinium to α-subunit residue atoms is also evident, notably to the carbonyl oxygen of α-Ile346, and a similar dual role for this residue is likely (Nadanaciva *et al.*, 1999c).

Speculation: Links between the Transition State, ATP Binding, and Subunit Rotation

The foregoing discussion draws attention to the possibility that mechanical events occurring in the catalytic sites at the catalytic α/β interface during ATP hydrolysis, at the steps of formation, stabilization, and breakdown of the transition state, are linked to rotation of γ subunit. Formation of the pentacovalent intermediate will generate negative charge, drawing positive side chains into the site; subsequent collapse of the transition state will generate mutually repulsive Mg-ADP and P_i, which will move apart and take engaged side chains with them. Side chains that are linked both to reactants and to α subunit residues could force larger domain movements to occur involving initially the α/β interface and then α subunits.

The possible role of binding of Mg-ATP to the catalytic site comprised by the "open" (β_E) β subunit as a driving force for rotation of γ has also been discussed (Wang and Oster, 1998; Masaike *et al.*, 2000). Binding of Mg-ATP to this site is expected to close the β_E subunit, partly or fully, by an upward hinging of the C-terminal domain, and might initiate γ-rotation during ATP hydrolysis through β/γ subunit interactions. Functional interactions between regions of β and γ subunits are well established and shown to be required for rotational coupling (Nakamoto *et al.*, 1999). However the affinity of the β_E site is expected to be relatively low (K_d ~100 μM),

since this is presumably the site of lowest affinity. Thus the energy available from the binding event alone is relatively small. Binding of Mg-ATP to the highest affinity site (unisite catalysis) does not elicit rotation (Garcia and Capaldi, 1998). Thus, binding of Mg-ATP may be a factor, but it cannot be the only factor, in generating subunit rotation.

A speculative temporal sequence could be as follows. Enzyme that has just released product Mg-ADP has two catalytic sites filled and the low-affinity site is empty. (1) Binding of Mg-ATP to the empty catalytic site (β_E) causes a conformational change in this β subunit and sets off a partial γ rotation, such that γ moves and changes its aspect toward α subunits. (2) Acceleration of hydrolysis occurs as a conformational change of the α subunit at the α/β interface propels α-Arg376 into the catalytic site, completing the transition state for V_{max} Mg-ATP hydrolysis. (3) Collapse of the transition state generates Mg-ADP and P_i, which move away from each other. Residues α-Arg376 and β-Arg182 move with the P_i and, engaged in H-bond contact with α subunit residues, move α away from β. (4) Conformational torsion in α subunits is transmitted to γ, and moves γ to complete a 120° arc. Release of products to form an empty site is required at this step and is thus accelerated when rotation occurs.

ACKNOWLEDGMENT

This work was supported by NIH grant GM25349 to AES.

REFERENCES

Abrahams, J. P., Leslie, A. G. W., Lutter, R., and Walker, J. E. (1994). *Nature (London)* **370**, 621–628.
Al-Shawi, M. K., and Senior, A. E. (1992). *Biochemistry* **31**, 878–885.
Bianchet, M. A., Hullihen, J., Pedersen, P. L., and Amzel, L. M. (1998). *Proc. Natl. Acad. Sci. USA* **95**, 11065–11070.
Braig, K., Menz, R. I., Montgomery, M. G., Leslie, A. G. W., and Walker J. E. (2000). *Structure*, **8**, 567–573.
Coleman, D. E., Berghuis, A. M., Lee, E., Linder, M. E., Gilman, A. G., and Sprang, S. R. (1994). *Science* **265**, 1405–1412.
Dey, S., Ramachandra, M., Pastan, I., Gottesman, M. M., and Ambudkar, S. V. (1997). *Proc. Natl. Acad. Sci. USA* **94**, 10594–10599.
Dou, C., Grodsky, N. B., Matsui, T., Yoshida, M., and Allison, W. S. (1997). *Biochemistry* **36**, 3719–3727.
Fisher, A. J., Smith, C. A., Thoden, J. B., Smith, R., Sutoh, K., Holden, H. M., and Rayment, I. (1995). *Biochemistry* **34**, 8960–8972.
Garcia, J. J., and Capaldi, R. A. (1998). *J. Biol. Chem.* **273**, 15940–15945.
Guex, N., and Peitsch, M. C. (1997). *Electrophoresis*, **18**, 2714–2723.
Gopal, D., and Burke, M. (1995). *J. Biol. Chem.* **270**, 19282–19286.
Henry, G. D., Maruta, S., Ikebe, M., and Sykes, B. D. (1993). *Biochemistry*, **32**, 10451–10456.
Issartel, J. P., Dupuis, A., Lunardi, J., and Vignais, P. V. (1991). *Biochemistry* **30**, 4726–4733.
Kato-Yamada, Y., Noji, H., Yasuda, R., Kinosita, K., and Yoshida, M. (1998). *J. Biol. Chem.* **273**, 19375–19377.
Ko, Y. H., Bianchet, M., Amzel, L. M., and Pedersen, P. L. (1997). *J. Biol. Chem.* **272**, 18875–18881.
Le, N. P., Omote, H., Wada, Y., Al-Shawi, M. K., Nakamoto, R. K., and Futai, M. (2000). *Biochemistry* **39**, 2778–2783.
Löbau, S., Weber, J., and Senior, A. E. (1998). *Biochemistry* **37**, 10846–10853.
Lunardi, J., Dupuis, A., Garin, J., Issartel, J. P., Michel, L., Chabre, M., and Vignais, P. V. (1988). *Proc. Natl. Acad. Sci. USA* **85**, 8958–8962.
Maruta, S., Henry, G. D., Sykes, B. D., and Ikebe, M. (1993). *J. Biol. Chem.* **268**, 7093–7100.
Maruta, S., Homma, K., and Ohki, T. (1998). *J. Biochem.* **124**, 578–584.
Masaike, T., Mitome, N., Noji, H., Muneyuki, E., Yasuda, R., Kinosita, K., and Yoshida, M. (2000). *J. Exp. Biol.* **203**, 1–8.
Nadanaciva, S., Weber, J., and Senior, A. E. (1999a). *J. Biol. Chem.* **274**, 7052–7058.
Nadanaciva, S., Weber, J., and Senior, A. E. (1999b). *Biochemistry* **38**, 7670–7677.
Nadanaciva, S., Weber, J., Wilke-Mounts, S., and Senior, A. E. (1999c). *Biochemistry* **38**, 15493–15499.
Nadanaciva, S., Weber, J., and Senior, A. E. (2000). *Biochemistry* **39**, 9583–9590.
Nakamoto, R. K., Ketchum, C. J., and Al-Shawi, M. K. (1999). *Annu. Rev. Biophys. Biomol. Struct.* **28**, 205–234.
Noji, H., Yasuda, R., Yoshida, M., and Kinosita, K. (1997). *Nature (London)* **386**, 299–302.
Pänke, O., Gumbiowski, K., Junge, W., and Engelbrecht, S. (2000). *FEBS Lett.* **472**, 34–38.
Park, S., Ajtai, K., and Burghardt, T. P. (1997). *Biochemistry* **36**, 3368–3372.
Ramachandra, M., Ambudkar, S. V., Chen, D., Hrycyna, C. A., Dey, S., Gottesman, M. M., and Pastan, I. (1998). *Biochemistry* **37**, 5010–5019.
Rayment, I. (1996). *J. Biol. Chem.* **271**, 15850–15853.
Rees, D. C., and Howard, J. B. (1999). *J. Mol. Biol.* **293**, 343–350.
Rittinger, K., Walker, P. A., Eccleston, J. F., Smerdon, S. J., and Gamblin, S. J. (1997). *Nature (London)* **389**, 758–762.
Sambongi, Y., Iko, Y., Tanabe, M., Omote, H., Iwamoto-Kihara, A., Ueda, I., Yanagida, T., Wada, Y., and Futai, M. (1999). *Science* **286**, 1722–1724.
Scheffzek, K., Ahmadian, M. R., Kabsch, W., Wiesmuller, L., Lautwein, A., Schmitz, F., and Wittinghofer, A. (1997). *Science* **277**, 333–338.
Schindelin, H., Kisker, C., Schlessman, J. L., Howard, J. B., and Rees, D. C. (1997) *Nature (London)* **387**, 370–376.
Schlichting, I., and Reinstein, J. (1997). *Biochemistry* **36**, 9290–9296.
Schlichting, I., and Reinstein, J. (1999). *Nature Struct. Biol.* **6**, 721–723.
Senior, A. E., Al-Shawi, M. K., and Urbatsch, I. L. (1995). *FEBS Lett.* **377**, 285–289.
Senter, P., Eckstein, F., and Kagawa, Y. (1983). *Biochemistry* **22**, 5514–5518.
Smith, C. A., and Rayment, I. (1996). *Biochemistry* **35**, 5404–5417.
Sondek, J., Lambright, D. G., Noel, J. P., Hamm, H. E., and Sigler, P. B. (1994). *Nature (London)* **372**, 276–279.
Tesmer, J. J. G., Berman, D. M., Gilman, A. G., and Sprang, S. R., (1997). *Cell* **89**, 251–261.
Tsunoda, S. P., Aggeler, R., Noji, H., Kinosita, K., Yoshida, M., and Capaldi, R. A. (2000). *FEBS Lett.* **470**, 244–248.
Wang, H., and Oster, G. (1998). *Nature (London)* **398**, 279–282.
Webb, M. R., Grubmeyer, C., Penefsky, H. S., and Trentham, D.R. (1980). *J. Biol. Chem.* **256**, 11637–11639.
Weber, J., and Senior, A. E. (2000). *Biochim. Biophys. Acta*, **1458**, 300–309.
Weber, J., and Senior, A. E. (1997). *Biochim. Biophys. Acta* **1319**, 19–58.
Weber, J., Hammond, S. T., Wilke-Mounts, S., and Senior, A. E. (1998). *Biochemistry* **37**, 608–614.
Weber, J., Wilke-Mounts, S., Lee, R. S. F., Grell, E., and Senior, A. E. (1993). *J. Biol. Chem.* **268**, 20126–20133.
Xu, Y. W., Morera, S., Janin, J., and Cherfils, J. (1997). *Proc. Natl. Acad. Sci. USA* **94**, 3579–3583.